# Root Bending Is Antagonistically Affected by Hypoxia and ERF-Mediated Transcription via Auxin Signaling[1][OPEN]

**Emese Eysholdt-Derzsó and Margret Sauter[2]**

Plant Developmental Biology and Plant Physiology, University of Kiel, 24118 Kiel, Germany

**ORCID ID: 0000-0002-7370-643X (M.S.).**

When plants encounter soil water logging or flooding, roots are the first organs to be confronted with reduced gas diffusion resulting in limited oxygen supply. Since roots do not generate photosynthetic oxygen, they are rapidly faced with oxygen shortage rendering roots particularly prone to damage. While metabolic adaptations to low oxygen conditions, which ensure basic energy supply, have been well characterized, adaptation of root growth and development have received less attention. In this study, we show that hypoxic conditions cause the primary root to grow sidewise in a low oxygen environment, possibly to escape soil patches with reduced oxygen availability. This growth behavior is reversible in that gravitropic growth resumes when seedlings are returned to normoxic conditions. Hypoxic root bending is inhibited by the group VII ethylene response factor (ERFVII) RAP2.12, as *rap2.12-1* seedlings show exaggerated primary root bending. Furthermore, overexpression of the ERFVII member *HRE2* inhibits root bending, suggesting that primary root growth direction at hypoxic conditions is antagonistically regulated by hypoxia and hypoxia-activated ERFVIIs. Root bending is preceded by the establishment of an auxin gradient across the root tip as quantified with DII-VENUS and is synergistically enhanced by hypoxia and the auxin transport inhibitor naphthylphthalamic acid. The protein abundance of the auxin efflux carrier PIN2 is reduced at hypoxic conditions, a response that is suppressed by RAP2.12 overexpression, suggesting antagonistic control of auxin flux by hypoxia and ERFVII. Taken together, we show that hypoxia triggers an escape response of the primary root that is controlled by ERFVII activity and mediated by auxin signaling in the root tip.

Flooding is a common cause of hypoxia or anoxia in plants. Soil water logging and flooding are first encountered by roots, which respond to hypoxic conditions with metabolic adaptations, formation of aerenchyma, or formation of barriers to the radial loss of oxygen, that is, the reinforcement of the rhizodermis (Abiko et al., 2012; Sauter, 2013; Voesenek and Bailey-Serres, 2015). The AP2/ERF (apetala2/ethylene response factor) transcription factor family of Arabidopsis (*Arabidopsis thaliana*) has 147 members that can be subdivided into ten groups (Nakano et al., 2006). Members of group VII (short ERFVIIs) were identified as key regulators of low oxygen responses in Arabidopsis (Bailey-Serres et al., 2012; van Dongen and Licausi, 2015). ERFVII proteins are characterized by a conserved motif at the amino terminus that initiates protein degradation at normoxic conditions via the N-end rule pathway (Gibbs et al., 2011; Licausi et al., 2011). At reduced oxygen levels, ERFVIIs are stabilized and engage in transcriptional regulation of hypoxia-responsive genes (Mustroph et al., 2009, 2010). A significant number of hypoxia-regulated genes in plants encode for enzymes of anaerobic metabolism such as alcohol dehydrogenase and lactate dehydrogenase. Fermentation and other metabolic adjustments ensure energy supply required to maintain cellular integrity in times when mitochondrial respiration is impaired. Plants, however, not only maintain basic cellular functions at low oxygen conditions, but they also invest resources to support developmental reprogramming. These are often but not always driven by ethylene that accumulates in flooded tissue (Sauter, 2013; Loreti et al., 2016).

In this study, we investigated developmental adaptation of the root system to hypoxia. Root architecture is determined by the rates of adventitious and lateral root formation, by primary and lateral root growth rates, and by the angles at which roots grow. Some plants such as *Oryza sativa* and *Solanum dulcamara* that are adapted to frequent flooding grow adventitious roots when submerged to replace soil-borne roots that become dysfunctional (Sauter, 2013; Dawood et al., 2014). However, not all plants are programmed to readily form adventitious roots upon flooding. We therefore hypothesized that such plants may adapt their root system to low oxygen conditions by alternative strategies.

[1] This work was supported by the Deutsche Forschungsgemeinschaft.

[2] Address correspondence to msauter@bot.uni-kiel.de.

The author responsible for distribution of materials integral to the findings presented in this article in accordance with the policy described in the Instructions for Authors (www.plantphysiol.org) is: Margret Sauter (msauter@bot.uni-kiel.de).

M.S. conceived the project and supervised the experiments; E.E.D. and M.S. designed the experiments; E.E.D. performed and analyzed the experiments; and M.S. wrote the manuscript with contributions from E.E.D.

[OPEN] Articles can be viewed without a subscription.

www.plantphysiol.org/cgi/doi/10.1104/pp.17.00555

 

We employed Arabidopsis as a model plant to study developmental adaptation of roots to hypoxia and to investigate the role of ERFVIIs in root adaptation. Our studies revealed that ERFVII-dependent and ERFVII-independent hypoxia signaling control root structure by altering auxin activity.

Auxin determines root architecture by regulating growth rate, lateral root formation, and root growth direction. Auxin is a unique plant hormone in that its transport occurs in a polar manner, thereby providing a mechanism to actively generate auxin gradients. Indole-3-acetic acid (IAA), the main natural auxin in plants, is transported from cell to cell. IAA is protonated in the acidic apoplast and deprotonated in the weakly basic cytosol. Uptake of the uncharged molecule occurs by AUX1/LAX (auxin1/like AUX1) uptake carriers (Péret et al., 2012) in an undirected way. Extrusion of negatively charged IAA occurs via undirected ABCB transporter-mediated efflux (Noh et al., 2001; Geisler et al., 2005) and by PIN (pin-formed) proteins that are responsible for directed auxin movement (Friml et al., 2003; Blilou et al., 2005). The Arabidopsis genome codes for eight PIN proteins (Friml et al., 2003). Three of these, PIN 5, PIN6, and PIN8, are localized at the ER membrane and engage in intracellular auxin transport (Adamowski and Friml, 2015). PIN1, PIN2, PIN3, PIN4, and PIN7 are localized at the plasma membrane where they support polar auxin transport. In roots PIN1, PIN3, PIN4, and PIN7 are found at the lower, root tip-facing end of cells where they drive acropetal auxin transport. PIN2 is localized at the upper side of root epidermal cells and ensures basipetal auxin movement away from the root apex toward the base. Together, the auxin transporters drive the so-called reverse fountain movement of auxin, which describes auxin transport in the central cylinder toward the tip, redistribution to the sides in the root cap, and transport toward the base in the lateral root cap and epidermis (Blilou et al., 2005). Tropic responses such as root gravitropism result from asymmetric auxin distribution across the root that can be established when movement of auxin to the elongation zone is higher on one side than the other. While AUX1/LAX transporters determine auxin levels, directional auxin transport is driven by PIN proteins (Band et al., 2014).

In this study, we describe a change in root growth direction in response to hypoxia. Our analyses showed that root slanting is subject to regulation by ERFVIIs and functionally linked to polar auxin transport, revealing a role for auxin in hypoxia adaptation.

## RESULTS

### Expression of *HRE2* in Hypoxic Roots

To gain insight into the role of the oxygen-sensing subgroup VII AP2/ERFs (abbreviated ERFVIIs) in regulating root development, we employed promoter:GUS lines to study expression of *HRE2* in roots at normoxic and hypoxic conditions (Fig. 1, A–E). No activity was observed in roots of *HRE2:GUS5* seedlings at normoxic conditions (Fig. 1A). After exposure to 2% oxygen for 1 d, GUS staining was observed close to the root tip in the developing vasculature (Fig. 1, B–D). A similar pattern was visible in lateral roots (Fig. 1E). Induction of gene expression at hypoxic conditions indicated that HRE2 may mediate root adaptation specifically to low oxygen conditions. By contrast, expression of *HRE1* was induced by low oxygen and in response to ethylene (Hess et al., 2011; Supplemental Fig. S1).

### Hypoxia Induces Root Slanting

To study root development during hypoxia, we used seedlings grown for 6 d at long-day conditions on plates placed at a near-vertical angle and transferred them to the dark for 3 d to avoid photosynthetic oxygen evolution either at normoxic (21% $O_2$) or hypoxic (2% $O_2$) conditions (Fig. 2A). Exposure of wild-type seedlings to 2% $O_2$ caused slanting of the primary root (Fig. 2B). The primary root of seedlings kept at normoxic conditions grew downward with an average deviation of about 14° from the vertical (Fig. 2C). Exposure to hypoxia caused seedling roots to change growth direction within about 12 h. On average, the angle increased to 38.7° after 3 d of hypoxia.

We hypothesized that the change in growth direction of the primary root at low oxygen conditions was not simply due to a reduced energy supply but was a developmentally regulated process. To test that hypothesis,

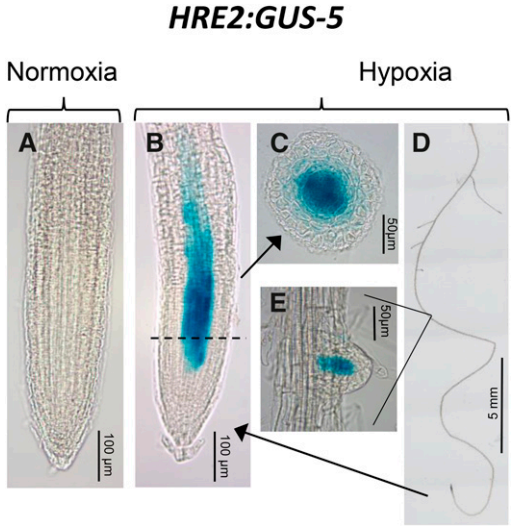


**Figure 1.** *HRE2:GUS* expression is induced by hypoxia in the developing stele. Histochemical GUS analysis of 7-d-old *HRE2:GUS-5* seedlings that were exposed to (A) normoxic (21% $O_2$) or (B–E) hypoxic (2% $O_2$) conditions for 1 d. A, Normoxic primary root tip. B, Hypoxic primary root tip. C, Cross-section through primary root tip as indicated in B. D, Hypoxic root. E, Hypoxic lateral root after emergence.

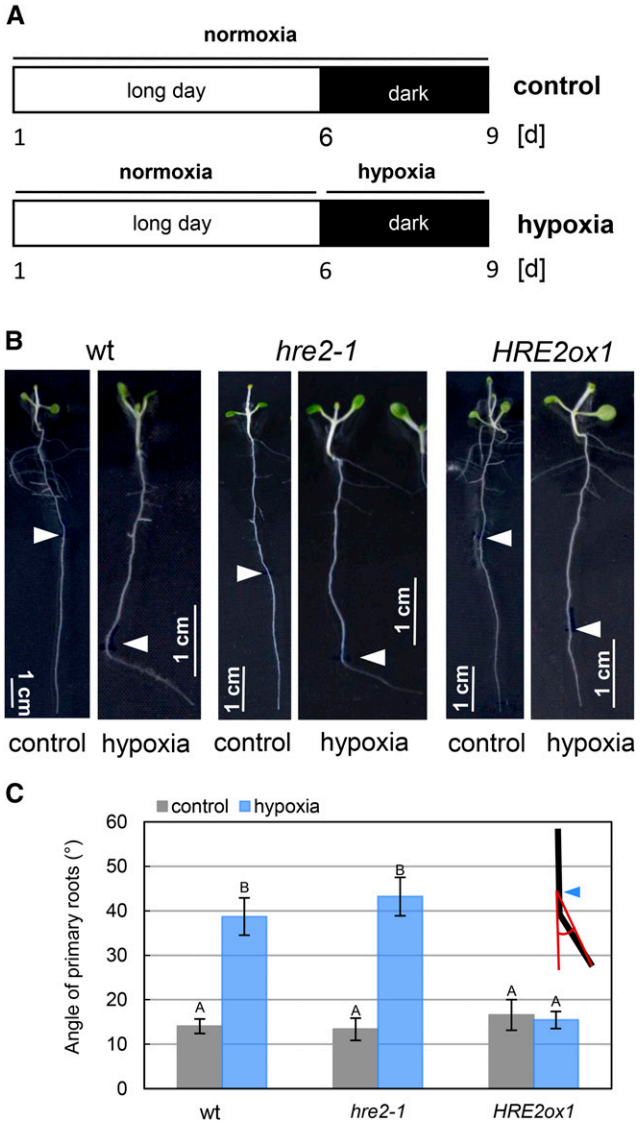


**Figure 2.** Hypoxia alters primary root growth direction. A, Six-d-old light-grown seedlings were transferred to the dark at control (21% $O_2$) or hypoxic (2% $O_2$) conditions for 3 d. B, Representative roots of 9-d-old wild-type, *hre2-1* and *HRE2ox1* seedlings exposed to the treatment protocols shown in A. Arrowheads indicate the position of the root tip at the beginning of the hypoxia treatment. C, Average angles by which the primary root changed its growth direction in the three genotypes exposed to normoxia or hypoxia. Results are averages (± SE) from three independent experiments. Different letters indicate significantly different values (Kruskal-Wallis test with Dunn's test, $n = 24–30$, $P < 0.05$). Insert: schematic showing how the angles were determined. The blue arrowhead indicates the position of the root tip at time of transfer.

we explored the involvement of ERFVIIs in regulating the slanting response. Since *HRE2* was induced in roots upon hypoxia, we employed *HRE2* knockout and overexpression lines to study an HRE2 function in slanting. Six-day-old seedlings were exposed to 3 d of hypoxia or to ambient oxygen conditions in the dark (Fig. 2A). The *hre2-1* knockout line (Supplemental Fig. S2; Hess et al., 2011) showed wild-type slanting, whereas *HRE2ox1* seedlings had lost their ability to change root growth direction in response to low oxygen (Fig. 2, B and C), suggesting that slanting was repressed by ERFVIIs. The observation that root slanting was not increased in *hre2-1* seedlings suggested that ERFs other than HRE2 might naturally regulate root growth direction.

To test the contribution of other ERFVIIs in the control of root slanting, we compared the slanting response in knockout mutants of *RAP2.3*, *RAP2.12*, *HRE1*, *HRE2*, the double knockout line *hre1-1 hre2-1* and the quintuple knockout line *erfVII* (Abbas et al., 2015; Fig. 3). For RAP2.2, a true knockout is not available. It was therefore not analyzed. The gene models with the insertion sites of the T-DNA are shown in Supplemental Figure S2. Loss of gene expression in the knockout lines was verified by reverse transcription-PCR (RT-PCR). Compared to wild type, *rap2.12-1* seedlings displayed significantly increased root bending (Fig. 3) with a mean angle of 70.4°. A role of ERFVIIs in the suppression of hypoxia-induced root slanting was further supported by the exaggerated slanting phenotype of *erfVII* seedlings. Loss of ERFVIIs activity resulted in primary root growth that deviated from the gravity vector by a mean angle of 58.8°. Interestingly, while hypoxic *hre1-1*, *hre2-1*, and the *hre1-1 hre2-1* double knockout seedlings did not have a significantly different root growth angle compared to wild type, they did slant significantly less than *rap2.3-2* and *rap2.12-1* seedlings, indicating that the function of RAP2.3 and RAP2.12 is not fully redundant to that of HRE1 and HRE2. The data further suggested that RAP2.12 plays a key role in controlling root bending.

Imposing alternating hypoxic and normoxic conditions (Fig. 4A) revealed that primary root bending induced by hypoxia was reversible. Roots rapidly

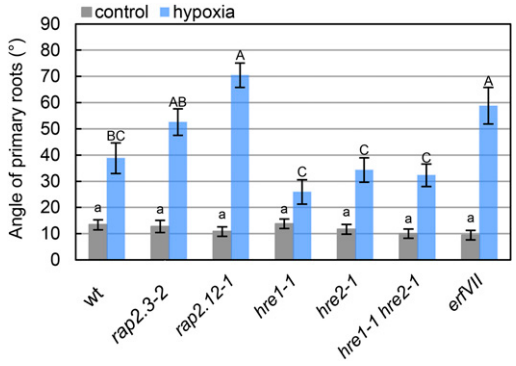


**Figure 3.** Root slanting at hypoxic conditions is negatively controlled by RAP2.12. Seedlings of wild type; the single gene knockout lines *rap2.3-2*, *rap2.12-1*, *hre1-1*, and *hre2-1*; the double knockout line *hre1-1 hre2-1*, and the quintuple knockout line *erfVII* were exposed to hypoxic conditions as indicated in Figure 2A. Subsequently, the angle by which roots deviated from the original growth direction was determined. Results are averages (± SE) from three independent experiments. Lowercase a indicates no difference between genotypes at normoxic (control) conditions; different capital letters indicate significant differences between genotypes at hypoxic conditions (Kruskal-Wallis test with Dunn's test, $n = 25–29$, $P < 0.05$).

returned to gravitropic growth when transferred from hypoxic to normoxic conditions and resumed slanting during a second hypoxic phase (Fig. 4B), suggesting that agravitropic root growth in response to oxygen limitation is a tightly regulated and reversible process.

### Hypoxia Triggers Asymmetric Auxin Distribution at the Root Apex

According to the Cholodny-Went theory, directed growth of plant organs such as phototropic or gravitropic growth is the result of an auxin gradient that is established across the organ (Briggs, 2014). To test if hypoxia alters auxin levels we employed the DII-VENUS reporter line to study auxin activity at the root tip (Fig. 5). The DII-VENUS protein is degraded as a consequence of $SCF^{TIR1}$-mediated auxin signaling (Brunoud et al., 2012). The DII-VENUS fluorescence was visualized by confocal laser scanning microscopy (Fig. 5A). It decreased when seedlings were exposed to 2% oxygen for 7 h compared to control seedlings kept in air, indicating that auxin activity was elevated (Fig. 5, A and B). Furthermore, the distribution of the fluorescence across the root became significantly more asymmetric at hypoxic conditions revealing an auxin gradient (Fig. 5, A and C).

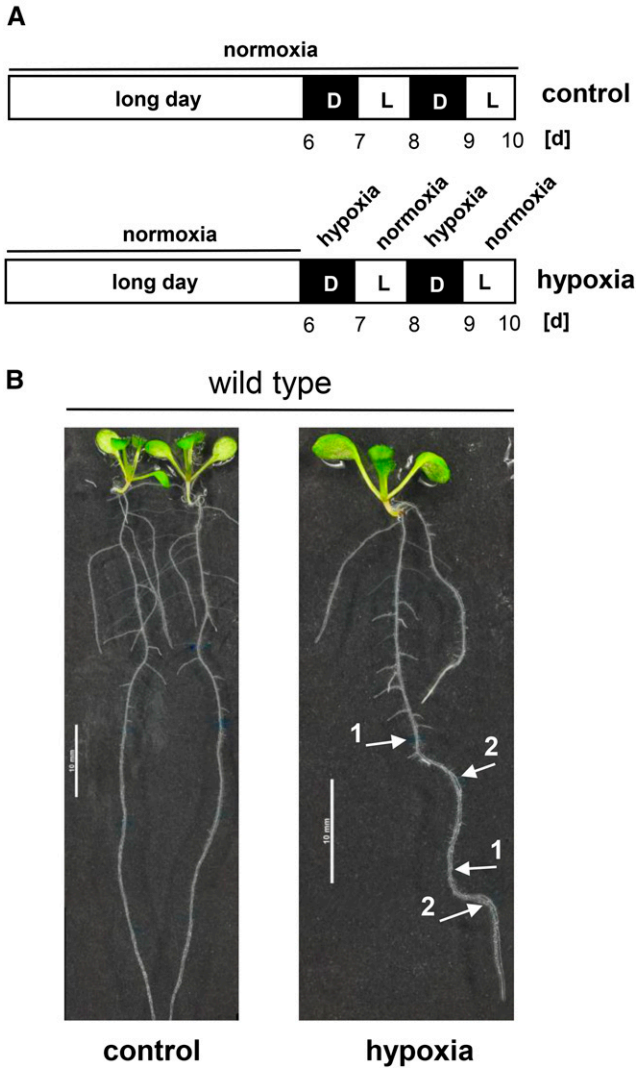


**Figure 4.** Hypoxia-induced slanting is a reversible growth response. A, Six-d-old seedlings were alternately exposed to hypoxic and normoxic conditions as indicated or kept at normoxic conditions as a control. B, Representative wild-type seedlings grown at normoxic conditions (control) or exposed to alternate normoxic and hypoxic conditions. Arrows indicate the position of the root tip at time of transfer to (1) hypoxia or (2) normoxia.

### Auxin Enhances Hypoxia-Induced Root Bending

To further test for a role of auxin in hypoxia-induced root slanting, we preincubated 5-d-old wild-type, *hre2-1*, and *HRE2ox1* seedlings (Supplemental Fig. S4) with the auxin analog $\alpha$-naphthalene acetic acid ($\alpha$-NAA) or the auxin transport inhibitor N-1-naphthylphthalamic acid (NPA; Geisler et al., 2005; Nishimura et al., 2012; Zhu et al., 2016) for 1 d followed by hypoxic treatment for another 2 d or by normoxic conditions as a control in the presence of auxin or NPA (Fig. 6A). In the presence of 20 nM $\alpha$-NAA, wild-type roots showed significantly increased bending even at normoxic conditions, with an average growth angle of 17.2° compared to 9.1° in the control (Fig. 6, B and C). In hypoxia, the average angle increased to 33.6° in wild type. $\alpha$-NAA and hypoxia caused bending at an angle of 55.1°. Root bending of wild-type seedlings was promoted by 0.5 $\mu$M NPA from 9.1° to 26.9° at normoxic and from 33.6° to 93.2° at hypoxic conditions. The response to NPA and hypoxia exceeded the responses to the single treatments, indicating that the two signals act in a synergistic manner pointing to a role of auxin transport in hypoxia-induced root slanting. *hre2-1* seedlings showed wild-type slanting behavior while slanting was reduced in *HRE2ox1* seedlings at hypoxic conditions but not fully inhibited when seedlings were exposed to auxin or NPA.

To further explore the link between hypoxia and auxin, we employed the *DR5:GUS* marker as a positive indicator for auxin activity. *DR5:GUS* seedlings were treated with 20 nM $\alpha$-NAA or 0.5 $\mu$M NPA or left untreated (Fig. 6, A and D). Treatment with $\alpha$-NAA increased auxin activity at the root apex. NPA enhanced auxin activity, particularly at the root apical meristem as described previously (Ottenschläger et al., 2003). At hypoxic conditions GUS activity increased likewise at the root apical meristem, a pattern that was even more pronounced when hypoxic seedlings were treated with NPA, further supporting the idea that auxin distribution is a target of hypoxia signaling. An asymmetric auxin distribution across the root tip was not observed in *DR5:GUS* seedlings, likely due to the lower sensitivity of this reporter as compared to the DII-VENUS reporter (Brunoud et al., 2012).

Our results revealed that root bending is synergistically enhanced by NPA and hypoxia, possibly suggesting that hypoxia signaling via ERFVII transcription factors targets auxin transport.

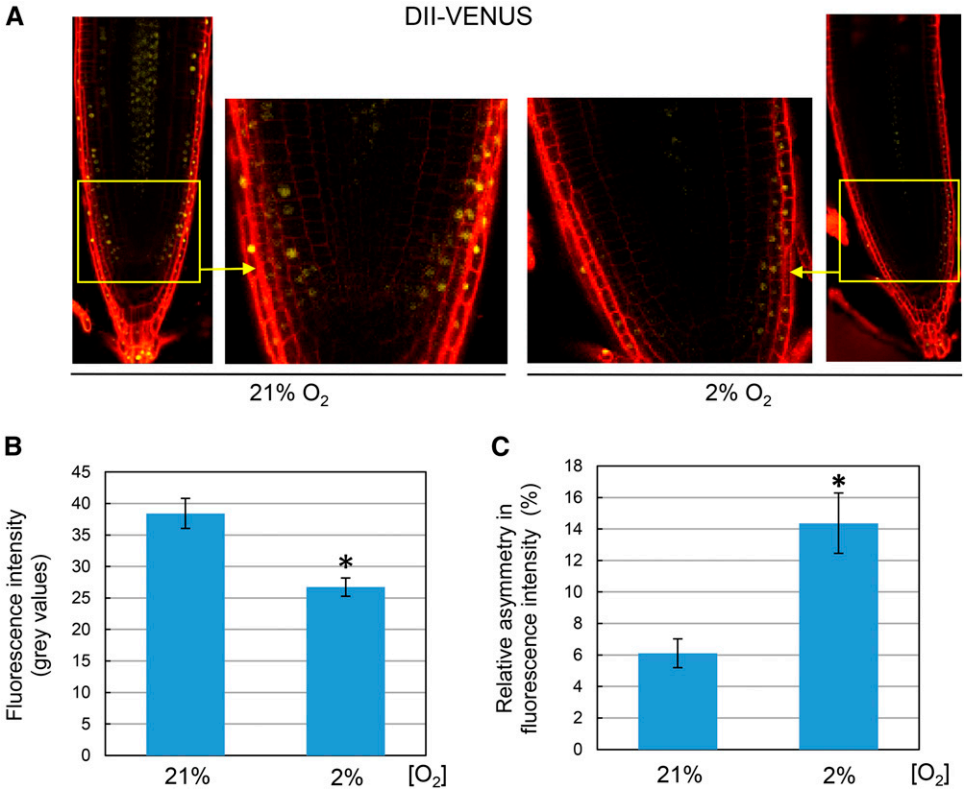


**Figure 5.** Hypoxia triggers asymmetric auxin distribution. A, Six-d-old DII-VENUS seedlings were exposed to normoxia or hypoxia for 7 h in the dark to examine auxin distribution at the root tip. B, Average (± SE) fluorescence intensities at the root tip were quantified in three independent experiments. The asterisk indicates a significantly reduced value at hypoxic conditions (two-sample *t* test, $n = 21–30$, $P < 0.05$). C, Relative average asymmetries (± SE) in fluorescence intensities between the two sides of the root tip. The asterisk indicates significantly different values (Mann-Whitney *U* test, $n = 21–30$, $P < 0.001$).

**PIN2 Protein Abundance Is Antagonistically Regulated by Hypoxia and RAP2.12**

Auxin distribution is an active process that is driven by auxin transporters. Since we observed local changes in auxin activity at hypoxic conditions and since NPA mimicked the auxin distribution at the root tip that was observed upon hypoxia, we hypothesized that hypoxia promotes root bending by acting on auxin transport proteins. Auxin transport is mediated by different auxin transport protein classes that include the PIN proteins that are responsible for polar auxin transport. To test the hypothesis that hypoxia promotes bending by altering polar auxin transport, we studied hypoxia-induced root bending in *pin1-1*, *pin2-1*, *pin3-4*, and *pin4-2* mutant seedlings.

Wild-type and *pin1-1*, *pin2-1*, *pin3-4*, and *pin4-2* knockout seedlings were pretreated with 20 nM α-NAA for 1 d or left untreated and subsequently transferred to 2% $O_2$ in the dark for hypoxic treatment or kept at normoxic conditions (for the treatment regime, see Fig. 6A). The phenotypes of the wild-type and PIN mutant seedlings are shown in Figure 7A. Subsequently, the angle of primary root growth direction was determined (Fig. 7B; Supplemental Fig. S5). As observed previously, hypoxia and auxin induced bending in the wild type that was exaggerated when both treatments were combined. Among the *pin* mutants, *pin1-1*, *pin3-4*, and *pin4-2* seedlings displayed wild-type root bending at all conditions. By contrast, the *pin2-1* mutant showed root slanting at normoxic conditions, with an average root growth angle of 26.8° as compared to 8.2° in wild type. However, neither hypoxia nor hypoxia in the presence of α-NAA further increased the angle at which *pin2-1* roots grew (Supplemental Fig. S5). These findings indicate that lack of PIN2, which is responsible for transport of auxin from the root tip toward its base, renders roots unresponsive to auxin and hypoxia with regard to their growth angle.

The PIN2 gene was not regulated by hypoxia, and expression of PIN2 was not altered in the erfVII mutant, indicating that PIN2 is not transcriptionally regulated during low oxygen conditions (Fig. 8A). To further study a possible role of PIN2 in hypoxia signaling, we looked at PIN2 protein distribution at the root tip of *PIN2pro:PIN2-GFP* seedlings at hypoxic conditions (Fig. 8). Confocal laser scanning microscopy confirmed PIN2 localization in the epidermis and cortex. The abundance of PIN2 protein decreased within 5 h of hypoxia as compared to controls (Fig. 8C), possibly indicating that reduced basipetal auxin transport via PIN2 may be responsible for increased auxin levels in these cells (Fig. 5). On the other hand, PIN2 distribution remained symmetrical up to 6 h of hypoxia (Fig. 8D). To answer the question if PIN2 protein was regulated not only by hypoxia but also by ERFVII signaling, we crossed the *PIN2pro:PIN2-GFP* line with wild type as a control and with RAP2.12 overexpressing line *RAP2.12 OE2* (Gasch et al., 2016). Reduced PIN2 abundance by hypoxia was confirmed in the *PIN2pro:PIN2-GFP* × wild-type line, whereas PIN2 was not reduced in

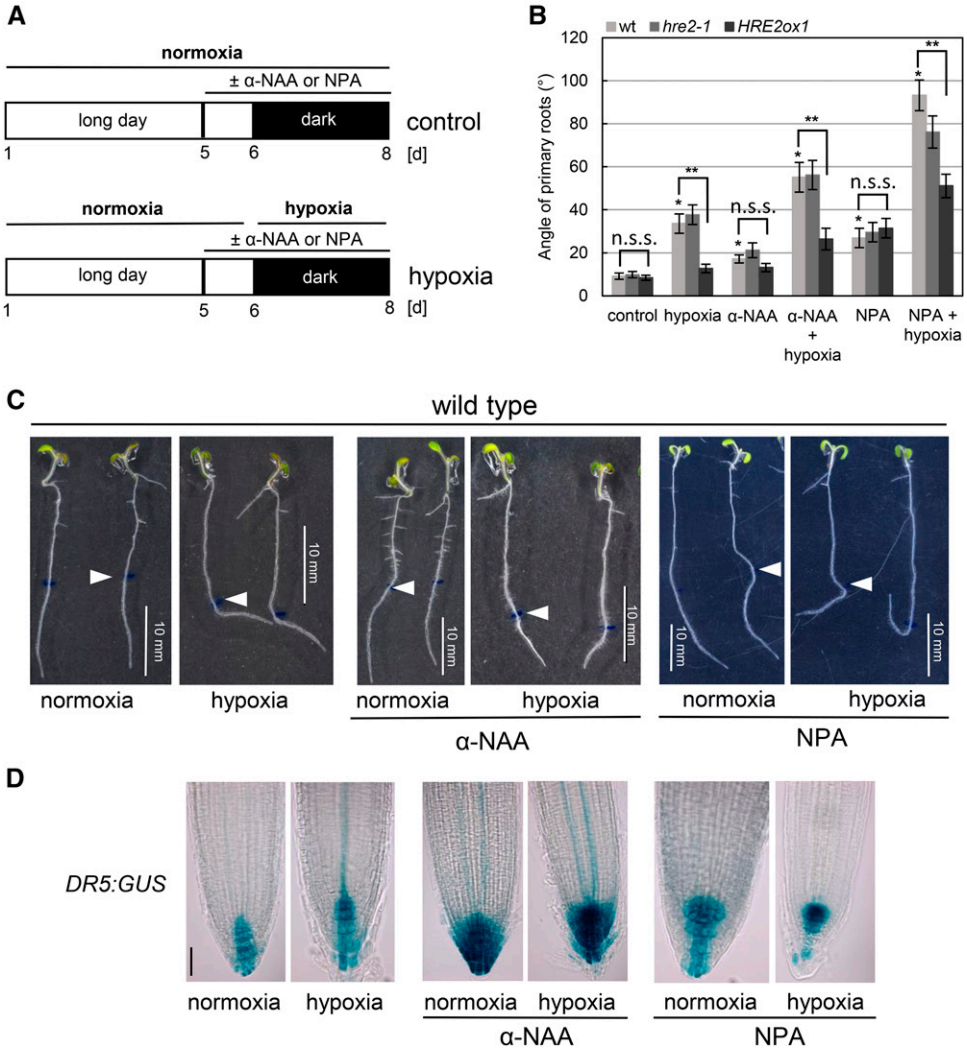


**Figure 6.** Root slanting is synergistically induced by hypoxia and the auxin transport inhibitor NPA. A, Treatment protocol: 6-d-old light-grown wild-type seedlings were pretreated with 20 nM α-NAA or 0.5 μM NPA and then transferred to the dark at control (21% $O_2$) or hypoxic (2% $O_2$) conditions for 2 d. B, Angles by which root growth direction deviate from the vertical vector were determined in three biological replicates. *Significant difference between control and treatment in wild type; **significant difference; n.s.s., no statistically significant difference between wild type and *HRE2ox1* (Mann-Whitney *U* test, $n = 22–30$, $P < 0.0001$). C, Representative roots of 8-d-old seedlings exposed to the treatments indicated in A. Arrowheads show the position of the root tip at the onset of the hypoxic treatment. D, Auxin activity at the root apex following the treatments indicated in A was visualized with the *DR5:GUS* reporter (bar = 50 μm; applies to all pictures).

*PIN2pro:PIN2-GFP* × *RAP2.12 OE2* seedlings (Fig. 8, E and F; Supplemental Fig. S6). Our data thus reveal an antagonistic effect of hypoxia and RAP2.12 on PIN2 protein abundance that may reflect a well-balanced control of auxin activity at the root apex at low oxygen conditions.

## DISCUSSION

### Hypoxia and ERFVIIs Antagonistically Regulate Primary Root Growth Direction

The ERFVII group of transcription factors has five members, RAP2.2, RAP2.3, RAP2.12, HRE1, and HRE2, that were shown previously to regulate hypoxic response genes (Licausi et al., 2010; Hess et al., 2011; Bui et al., 2015), prominently among which are genes involved in the metabolic shift from respiration to fermentation. More recently, however, RAP2.2 and RAP2.12 were identified as principle activators of hypoxia-responsive genes, while RAP2.3, HRE1, and HRE2 were shown to play minor roles (Gasch et al., 2016). The expression of the ERFVII members are differentially induced by environmental factors such as darkness, hypoxia, or ethylene (Hinz et al., 2010; Licausi et al., 2010; Hess et al., 2011), supporting the idea that ERFVII members have distinct physiological functions.

This study shows that Arabidopsis seedlings that encounter hypoxic conditions change the direction of primary root growth. This response is under negative control of ERFVIIs, as the quintuple *erfVII* mutant displays exaggerated root bending. A comparable phenotype was observed in *rap2-12-1* seedlings but not in *rap2.3-2*, *hre1-1*, and *hre2-1* seedlings, indicating that RAP2.12 acts to suppress root bending in response to hypoxic conditions. *HRE2* is expressed at low oxygen conditions in the developing vasculature at the root tip, but knockout of *HRE2* does not alter the slanting response of the primary root, indicating that ERFVII activity in the developing stele is not sufficient to change root growth direction. Yet, when expressed ectopically at high levels, HRE2 efficiently inhibited hypoxia-induced

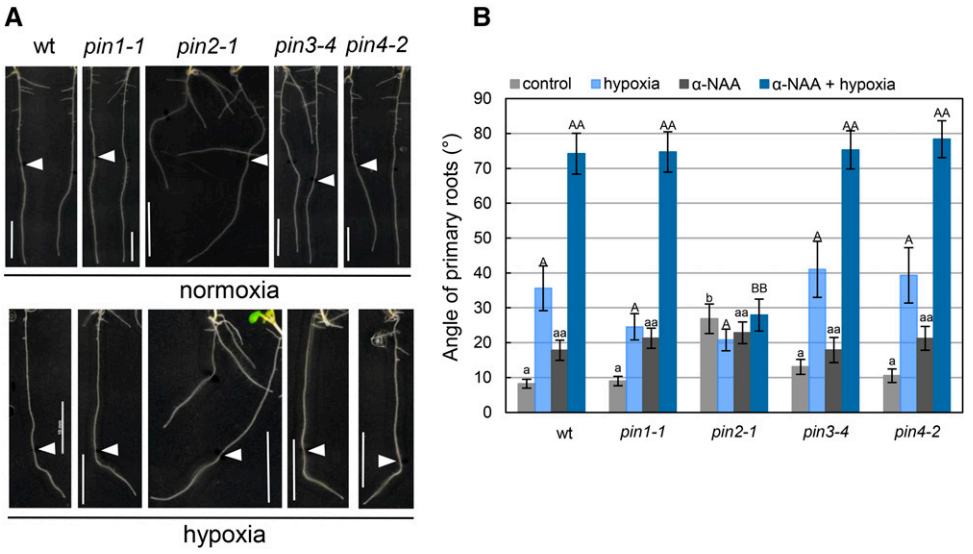


**Figure 7.** The *pin2-1* mutant is unresponsive to hypoxia and auxin. A, Representative root phenotypes of 8-d-old wild-type, *pin1-1*, *pin2-1*, *pin3-4*, and *pin4-2* seedlings grown at normoxic or hypoxic conditions for 2 d (bar = 10 mm). B, Average angles of primary root growth direction in wild type, *pin1-1*, *pin2-1*, *pin3-4* and *pin4-2* seedlings treated as indicated in Figure 6A. Different single minor letters indicate significantly different values in the control; different capital letters indicate significantly different values in hypoxia-treated seedlings; different double minor letters indicate significantly different values in seedlings treated with 20 nM α-NAA; different double capital letters indicate significantly different values in seedlings treated with 20 nM α-NAA at hypoxic conditions (Kruskal-Wallis test with Dunn's test, $n = 23–25$, $P < 0.01$). Results are averages (± SE) from three independent experiments. Statistically significant differences within a given genotype are shown in Supplemental Figure S5.

root bending, suggesting that it can function redundantly to RAP2.12 depending on its spatiotemporal expression.

Interestingly, hypoxia promotes slanting as well as stabilization of RAP2.12, which, in turn, inhibits slanting. In wild-type seedlings, the angle of hypoxia-induced root bending was intermediary to that observed in *HRE2ox1* and *rap2.12-1* or *erfVII* seedlings, indicating that the growth angle of hypoxic roots is regulated by ERFVII activity in a dose-dependent manner making ERFVIIs a potential hub for signal integration. Environmental signals other than the oxygen concentration might determine root growth direction by controlling RAP2.12 activity through transcriptional regulation, protein stability, or subcellular localization (Licausi et al., 2011; Kosmacz et al., 2015).

Slanting primary roots rapidly resumed gravitropic growth when seedlings were returned to normoxic conditions, indicating that the gravisensing mechanism was intact. Gravity sensing in roots is performed in root cap cells by amyloplasts that act as sedimenting statoliths (Baldwin et al., 2013). The molecular mechanism that underlies gravity perception is not understood. The signal is transmitted from the root cap statocytes via basipetal auxin transport to the root elongation zone mediated by the polar auxin transporter PIN2 (Müller et al., 1998). Differential auxin transport between the lower and upper sides of the root tip results in differential growth manifested as root bending. Hypoxia offsets gravitropic primary root growth while resupply of oxygen to normoxic levels restores it. Genetic data point to RAP2.12 as the major ERFVII that limits root slanting during hypoxia without fully inhibiting it, suggesting that slanting serves a physiological function. Primary root slanting might be an escape response that is induced by hypoxia and at the same time restricted by hypoxia-stabilized RAP2.12.

In nature, roots encounter hypoxic conditions due to soil water logging or flooding. If oxygen availability declines with soil depth, sidewise growth of the root may help to reach remaining gas spaces to maintain root oxygen supply. When the root is well supplied with oxygen positive gravitropic growth resumes to ensure anchoring and exploration of nutrients and water in deeper soil layers.

### ERFVII and Auxin Pathways Interact to Control Root Slanting

Application of α-NAA or NPA increased auxin activity at the root tip as detected by the *DR5:GUS* reporter. At the same time, the angle at which roots grew when exposed to hypoxia was exaggerated with auxin and NPA. NPA inhibits auxin flux primarily by inhibiting nonpolar ABCB19 auxin transporters and PIN-type auxin transporters, which results in a local increase in auxin concentration (Ottenschläger et al., 2003; Geisler et al., 2005; Nishimura et al., 2012; Habets and Offringa, 2014; Zhu et al., 2016). A synergistic effect of NPA and hypoxia and, to a lesser degree, of auxin and hypoxia was observed with regard to root bending, indicating that hypoxia and auxin signaling pathways

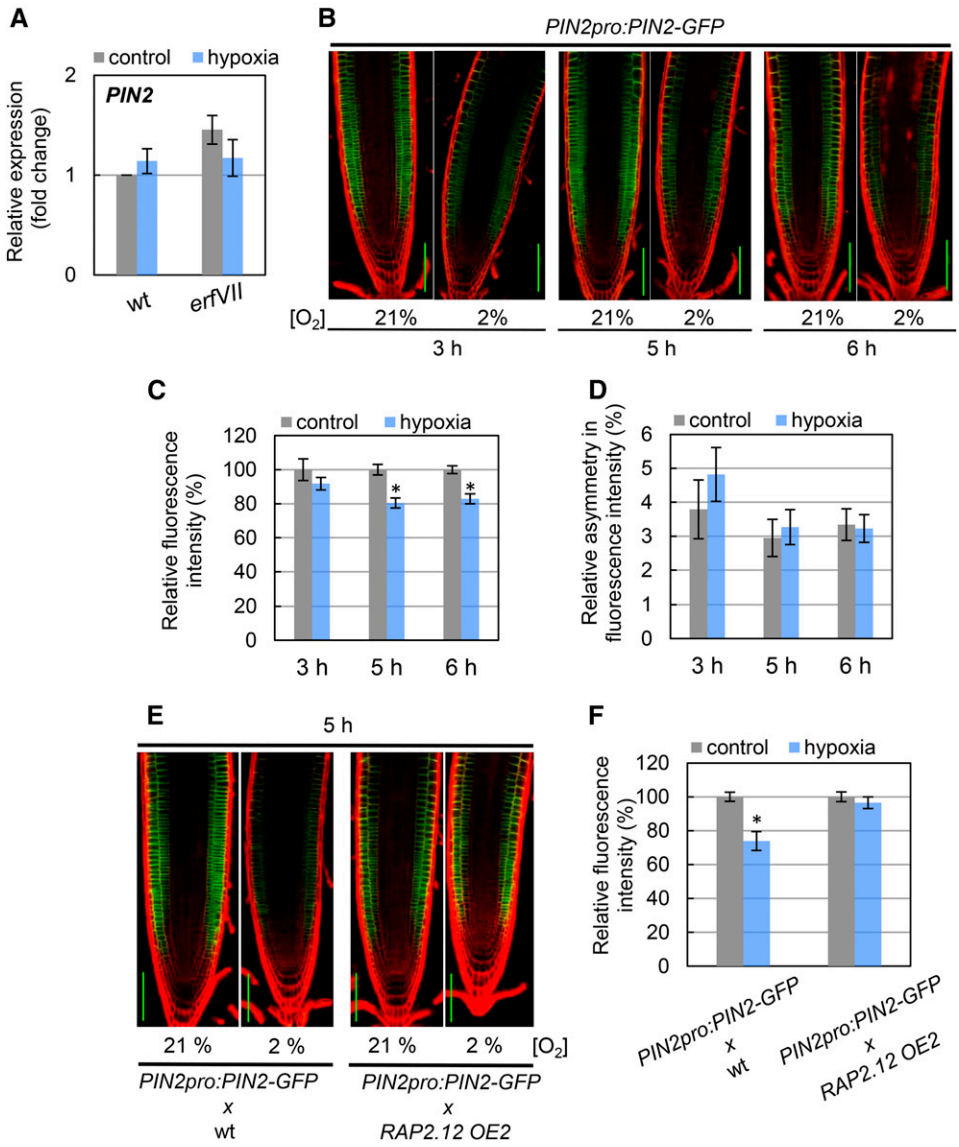


**Figure 8.** Hypoxia causes a decrease in PIN2 abundance at the root tip. A, Expression levels of *PIN2* in the root tips of 6-d-old wild-type and *erfVII* seedlings exposed to 21% $O_2$ (control) or 2% $O_2$ (hypoxia) for 8 h in the dark were quantified by quantitative RT-PCR. Results are means (± SE) of three independent biological replicates with two technical repeats each (one-way ANOVA with Tukey's test, $P < 0.05$). B, Visualization of PIN2-GFP at the root tip of 6-d-old *PIN2pro:PIN2-GFP* seedlings that were exposed to normoxia or hypoxia for 3, 5, or 6 h in the dark. Scale bar = 100 $\mu$m. C, Average (± SE) fluorescence intensities at the root tips of hypoxic seedlings were normalized to the control samples in three independent experiments. Asterisks indicate significantly different values (two-sample *t* test, $n = 18–20$, $P < 0.05$). D, PIN2-GFP fluorescence intensities across the root tip are not significantly different. Results are averages (± SE, $n = 18–20$) from three independent experiments. E, PIN2-GFP fluorecence in *PIN2pro:PIN2-GFP* × wild-type seedlings and in *PIN2pro:PIN2-GFP* × *RAP2.12 OE2* seedlings exposed to normoxic or hypoxic conditions. Scale bar = 100 $\mu$m. F, Quantification of relative PIN2-GFP fluorecences (± SE) in the root tips of *PIN2pro:PIN2-GFP* × wild type and *PIN2pro:PIN2-GFP* × *RAP2.12 OE2* seedlings reveal a regulatory role of RAP2.12 in PIN2 abundance at hypoxic conditions. The asterisk indicates a significant difference to the control (two-sample *t* test, $n = 14–17$, $P < 0.05$).

interact. Overexpression of *HRE2* fully repressed root bending at hypoxic conditions but only partially reduced root bending in response to auxin or NPA at hypoxic conditions, suggesting that elevated auxin activity can partly overcome ERFVIIs activity and may hence act downstream of ERFVIIs. The distribution of DR5:GUS activity at the root tip was altered in hypoxic as compared to normoxic conditions, pointing to auxin transport as a target of hypoxia signaling.

The DR5 reporter is based on multiple tandem repeats of a highly active synthetic auxin response element (AuxRE) that are fused upstream of a minimal 35S promoter-GUS reporter gene (Ulmasov et al., 1997). *DR5:GUS* expression does not directly indicate endogenous

auxin abundance but also depends on auxin signaling capacities and rates of transcription and translation, which may vary locally. The DII-VENUS reporter is based on the constitutive expression of a fusion protein of the auxin-binding domain (DII) of an Aux/IAA protein with the fluorescent VENUS protein (Brunoud et al., 2012). Binding of auxin to its receptor TIR1 results in degradation of DII-VENUS. Due to this immediate regulation by auxin, DII-VENUS fluorescence is directly related to endogenous auxin levels in that fluorescence decreases with elevated auxin abundance, and it is more sensitive than DR5:GUS activity. Analysis of the DII-VENUS reporter line confirmed increased auxin levels in root tips at hypoxic conditions and furthermore revealed asymmetric auxin distribution in the outer root cell layers. The lateral root cap and epidermis cells are the site of shootward auxin transport and were shown to be crucial for the gravitropic response (Swarup et al., 2005). Changes in auxin abundance and distribution in hypoxic conditions clearly suggest that hypoxia signaling affects auxin transport.

### Hypoxia Increases Auxin Activity at the Root Tip

Auxin movement from cell to cell is achieved by nonpolar auxin influx mediated by AUX1/LAX carriers and by auxin efflux carriers (Band et al., 2014). Auxin efflux is mediated by the nonpolar ABCB carriers and by the polar auxin efflux carriers PIN1, PIN2, PIN3, PIN4, and PIN7 (Habets and Offringa, 2014). AUX1/LAX carriers control auxin levels, while PINs control the direction of auxin transport within tissues (Band et al., 2014). Basipetal auxin transport in roots is mediated by PIN2 that is localized in the epidermis and cortex at the root apex (Wisniewska et al., 2006). In epidermal cells, PIN2 was shown to be localized to the upper side, whereas in cortex cells PIN2 is found at the basal side (Wisniewska et al., 2006). PIN2-GFP abundance decreased at hypoxic conditions. Reduced PIN2 protein abundance may limit basipetal auxin transport and thereby contribute to the increased auxin activity that we observed at the root tip with the DR5:GUS and DII-VENUS reporters in response to hypoxia. Elevated auxin activity at the root tip has been observed in the *pin2* mutant (Boonsirichai et al., 2003). Unlike other *pin* mutants that do not have an altered root gravitropic response, the *pin2* mutant shows weakly agravitropic root growth (Müller et al., 1998) that was also observed in this study. Hypoxia did not further increase the angle of agravitropic growth of the *pin2-1* mutant. Hypoxia and $\alpha$-NAA promoted root bending in a nonadditive manner in wild type but, again, did not enhance root slanting of *pin2-1* seedlings. All other PIN mutants, *pin1-1*, *pin3-4*, and *pin4-2*, showed a wild-type root growth phenotype in response to hypoxia. These data indicate that PIN2 acts epistatic to hypoxia.

Down-regulation of PIN2 protein by hypoxia and suppression of this down-regulation by RAP2.12 overexpression indicate that auxin activity at the root tip is actively controlled by modulation of PIN2 protein abundance. As elevated auxin activity at the root tip goes along with increased root bending (Fig. 6), we hypothesize that a decrease in PIN2 protein level reduces shootward auxin flux, causing auxin to accumulate at the apex, which promotes root bending (Fig. 9).

PIN2 is degraded by the ubiquitin-proteasome pathway in the vacuole (Abas et al., 2006; Leitner et al., 2012; Adamowski and Friml, 2015). Reduced PIN2 levels in roots exposed to hypoxia may indicate that hypoxia signaling targets the PIN2 protein degradation pathway. Baster et al. (2013) suggested that posttranslational regulation of PIN2 could lead to its proteasomal and vacuolar lytic degradation. The polar localization of PIN2 is regulated via phosphorylation by PINOID (PID) and its related protein kinases WAG1 and WAG2 that in turn are antagonized by protein phosphatase 2AA (Michniewicz et al., 2007; Adamowski and Friml, 2015; Santner and Watson, 2006). It is not shown here but conceivable that a similar regulatory mechanism targets PIN2 for degradation. Future work will have to unveil the mechanism by which hypoxia and RAP2.12 control PIN2 abundance.

The theory proposed by Cholodny and Went states that organ bending is caused by an auxin gradient across the organ. A difference in auxin levels across the root causes cells to elongate at different rates and the root to bend. However, while we did observe an auxin gradient, we did not observe an asymmetric distribution of PIN2 protein using the *PIN2pro:PIN2-GFP* reporter line. Since PIN2 distribution is highly dynamic, it is conceivable that polar PIN2 activity differentially changes at the two sides of the root in response to hypoxia and that we simply did not microscopically resolve this asymmetry. Alternatively, there is no PIN2 asymmetry and the auxin gradient is formed independent of PIN2 distribution.

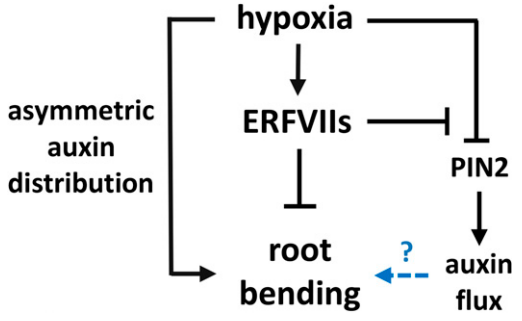


**Figure 9.** Model: Hypoxia signaling controls primary root growth direction in an ERFVII-dependent and ERFVII-independent manner. Hypoxia induces root bending by establishing an auxin gradient across the root tip, whereas hypoxia-stabilized EFVIIs limit root bending. The polar auxin transporter PIN2 is antagonistically regulated by hypoxia and RAP2.12 at the protein level, suggesting control of auxin flux. Both the hypoxia-induced lateral auxin gradient and reduced basipetal auxin flux alter local auxin activities that contribute to root bending.

## Conclusions

Arabidopsis seedlings adapt to hypoxic conditions by a change in root growth direction, possibly to explore gas spaces in the soil with higher oxygen levels. The angle of root bending is restricted by the activity of the oxygen-sensing ERFVII member RAP2.12 that gets activated at hypoxic conditions (Fig. 9). PIN2 is a polar auxin transporter that drives auxin transport from the root tip to the root elongation zone. Hypoxia reduces PIN2 abundance, promotes auxin activity at the root tip, and enhances root bending, whereas the hypoxia-stabilized RAP2.12 promotes PIN2 abundance and restricts root bending, indicating tight control of the slanting response. In summary, hypoxia induces root slanting by altering auxin signaling at the root apex.

## MATERIALS AND METHODS

### Plant Material

Experiments were carried out with Arabidopsis (*Arabidopsis thaliana*) Col-0 originally obtained from NASC. All mutants are in the Col-0 background with the exception of *pin1-1*, which is in the Enkheim background (Okada et al., 1991). The T-DNA insertion lines *hre1-1* (*erf73-1*) and *hre2-1* (*erf71-1*) were described previously (Hess et al., 2011) and were used to generate the double knockout line *hre1-1 hre2-1* by crossing. Knockout of both genes was verified by RT-PCR (Supplemental Fig. S1) in seedlings exposed to hypoxic conditions. The *pin1-1*, *pin4-2* (Gälweiler et al., 1998; Friml et al., 2002a, 2002b) lines were obtained with consent from J. Friml (Institute of Science and Technology Austria, Austria). *pin4-2* was verified as a homozygous EN-1 transposon line with the gene-specific primers AT2G01420for2 and AT2G01420rev2 (Supplemental Table S1). The *erfVII* line (Abbas et al., 2015) was kindly provided by M. J. Holdsworth (University of Nottingham), the DII-VENUS marker line (Brunoud et al., 2012) was kindly provided by Tom Beeckman (Ghent University), and the *DR5:GUS* line (Ulmasov et al., 1997) was obtained from T. Ulmasov (University of Missouri). *PIN2pro:PIN2-GFP* (Swarup et al., 2008) was a kind gift from Malcolm J. Bennett (University of Nottingham). The RAP2.12 OE2 line was kindly provided by Angelika Mustroph (University Bayreuth) and was described previously by Gasch et al. (2016). We crossed *PIN2pro:PIN2-GFP* with wild type and with *RAP2.12 OE2* to generate *PIN2pro:PIN2-GFP* × wild type and *PIN2pro:PIN2-GFP* × *RAP2.12 OE2* lines. The expression level of *RAP2.12* in wild type × *PIN2pro:PIN2-GFP* and *RAP2.12 OE2* x *PIN2pro:PIN2-GFP* seedlings was verified by RT-PCR (Supplemental Fig. S6) using the primers ForAT1G53910 and RevAT1G53910 (Supplemental Table S1).

The T-DNA insertion lines *rap2.3-2* (WiscDsLox247E11) described by Marín-de la Rosa et al. (2014), *rap.2.12-1* (GK_503A11) described by Gibbs et al. (2014), and *pin2-1* (GK_262G07-014951) and *pin3-4* (SALK_038609) described by Friml et al. (2003) were obtained from NASC and verified as homozygous knockout lines (Supplemental Figs. S1 and S3) with gene-specific and T-DNA insertion-specific primers (Supplemental Table S1) At3g16770For, At3g16770Rev, WisconDsLoxLB for *RAP2.3*, At1g53910For, At1g53910Rev, LB-GK for *RAP2.12*, At5g57090forRT, At5g57090revRT, LB-GK for *PIN2*, and AT1G70940forRT, AT1G70940revRT for *PIN3*.

### Growth Conditions and Analysis

Seeds were sterilized under continuous shaking (1,400 rpm) in 2% (w/v) sodium hypochlorite (Carl Roth) for 20 min at room temperature followed by three washing steps with sterilized ultra-pure water. Surface sterilized seeds were placed on square plates with 0.39% (w/v) gelrite (Duchefa), 1.5% (w/v) sucrose (Carl Roth), and half-strength Murashige and Skoog basal salt mix (Duchefa). For chemical treatments, 5-d-old seedlings were transferred to new plates supplemented with 0.5 $\mu$M NPA (Sigma) or 20 nM $\alpha$-NAA (Sigma) for 1 d prior to hypoxic treatment. Hypoxic treatment was carried out in the dark in airtight acryl boxes flushed at a flow rate of 2 L/min for $N_2$ and 40 mL/min with $O_2$ to equilibrate the atmosphere at 2% oxygen. To ensure that the oxygen concentrations in the acryl boxes were as desired, they were measured by gas chromatography at the beginning and end of the first treatment (Sasidharan et al., 2017). Controls were kept in acryl boxes in ambient air in the dark. Plates were placed upright leaning backward at an angle that deviated from the vertical by 6°. To measure the angle of primary root growth deviation, roots were imaged with an SMZ18 stereo microscope (Nikon) and a DS-U3 camera (Nikon) and analyzed with ImageJ (Schneider et al., 2012). The angles were measured between the growth direction of the primary root before transfer to normoxia or hypoxia in the dark and the line drawn from the position of the root tip at time of transfer to the position of the root tip at the end of the treatment as indicated in the cartoon in Figure 2C.

### Cloning and Plant Transformation

To generate *35S:HRE2* overexpressing lines, the open reading frame of *HRE2* was amplified by PCR with gene-specific primers (Supplemental Table S1, At2G47520 TC_forox, At2G47520 TC_revox primers) using cDNA isolated from seedlings exposed to hypoxia. The amplified fragment was cloned into the pENTR/D-Topo vector (Life Technologies) and subsequently recombined into the destination vector pB7WG2 using the Gateway cloning system (Karimi et al., 2002). This vector was transformed into *Agrobacterium tumefaciens* strain EHA105 followed by plant transformation of Col-0 with the floral dip method (Clough and Bent, 1998). T1 seeds were screened for glufosinate resistance and RNA was isolated from leaves of resistant plants. Transcript levels of *HRE2* and of *ACTIN2* as a control for RNA input were analyzed by RT-PCR with gene-specific primers (Supplemental Table S1; At2G47520forRT, At2G47520revRT, At2G47520forqPCR, and At2G47520revqPCR primers for *HRE2*; Actin2F1 and Actin2R1 primers for *Actin2*) using M-MuLV reverse transcriptase (Fermentas). Homozygous seeds were obtained after the T4 generation.

To generate *HRE2:GUS* lines, 728 bp 5′ of the start codon of *HRE2* was amplified from genomic DNA with promoter-specific primers (Supplemental Table S1, erf71profor, erf71prorev primers). The amplified promoter sequence was cloned into the pBGWFS7 destination vector (Karimi et al., 2002), transformed into *Agrobacterium* followed by plant transformation as described above. T1 seeds were screened for glufosinate resistance. Homozygous seeds were obtained after the T4 generation.

### Quantitative RT-PCR Analysis

To investigate the gene expression of *PIN2* in wild type and *erfVII*, 5 mm of the root tips was collected for RNA isolation. Gene expression was analyzed by qantitativeRT-PCR. The expression level in wild-type seedlings at control conditions was set to 1 and all other values are shown as multiples of that. *GAPC1* and *ACTIN2* were used for normalization. The primers AT5G57090qF and AT5G57090qR were used for the quantitative RT-PCR analysis of *PIN2*, Actin2qF and Actin2qR for *ACTIN2*, and GAPC1qF and GAPC1qR primers for *GAPC1* (Supplemental Table S1).

### Histochemical Analysis of Reporter Lines

Histochemical analysis of *HRE2:GUS* and *DR5:GUS* seedlings was performed according to Blázquez et al. (1997) with modifications. Plant material was directly collected into the $\beta$-glucuronidase staining solution (50 mM sodium-phosphate, 0.2% [v/v] Triton X-100, 2 mM $K_4[Fe(CN)_6]$, 2 mM $K_3[Fe(CN)_6]$, and 2 mM 5-brom-4-chloro-3-indolyl-glucuronide [Duchefa], pH 7.5). The *DR5:GUS* reporter line was incubated for 30 min and *HRE1:GUS* and *HRE2:GUS* seedlings were incubated for 2 h at 37C° and then stored in 70% (v/v) ethanol until analysis. To better visualize the blue staining, samples were cleared in a 6:2:1 (g/mL/mL) solution of chloralhydrate:deionized water:glycerol (Carl Roth). Cleared samples were mounted on a microscope slide and visualized with bright-field illumination using an Olympus BX41 (Olympus) microscope with Color View II Kamera.

### Microscopy and Live Imaging of DII-VENUS and PIN2-GFP

Six-day-old DII-VENUS seedlings were analyzed after 7 h of hypoxia treatment or treatment at normoxic conditions, and *PIN2pro:PIN2-GFP* seedlings were analyzed after 3, 5, or 6 h of hypoxia or normoxia by taking pictures with a confocal laser scanning microscope (Leica TCS SP5). Furthermore, PIN2 protein abundance was detected in root tips of wild type × *PIN2pro:PIN2-GFP* and *RAP2.12 OE2* × *PIN2pro:PIN2-GFP* seedlings after exposure to hypoxia or

normoxia for 5 h using confocal laser scanning microscopy. Fluorescence intensities in the plane of the quiescent center of each root tip were quantified with the LAS AF Lite software (Leica). The fluorescence intensities of PIN2-GFP at normoxic conditions were set to 100% and all other values are given in relation to that.

## Statistical Analysis

Statistical analyses were performed using Minitab14 software (www.minitab.com). A Student's *t* test (two-sample *t* test) was used to compare the means of two populations. One-way ANOVA with Tukey's post hoc test was applied for testing the variance of populations when they were normally distributed. The Kruskal-Wallis nonparametric one-way test was used to determine significant differences with Dunn's test for multiple comparisons among the group. A nonparametric Mann-Whitney *U* test was used for comparing two groups.

## Accession Numbers

Sequence data from this article can be found in the GenBank/EMBL data libraries under accession numbers RAP2.3 – At3g16770, RAP2.12 – At1g53910, HRE1 – At1g72360, HRE2 – At2g47520, PIN1 – At1g73590, PIN2 – At5g57090, PIN3 – At1g70940, and PIN4 – At2g01420.

## Supplemental Data

The following supplemental materials are available.

**Supplemental Figure S1.** Analysis of HRE1-GUS expression in response to low oxygen and ethylene.

**Supplemental Figure S2.** Gene models of RAP2.3, RAP2.12, HRE1, and HRE2 indicating the T-DNA insertion sites of the knockout lines used.

**Supplemental Figure S3.** Gene model of PINs with the T-DNA or EN-1 transposon insertion sites.

**Supplemental Figure S4.** Overexpression of HRE2 prevents root slanting at hypoxic conditions.

**Supplemental Figure S5.** Average angle of primary root growth direction in wild-type, pin1-1, pin2-1, pin3-4, and pin4-2 seedlings treated with 20 nM $\alpha$-NAA for 2 d at normoxic or hypoxic (2% $O_2$) conditions.

**Supplemental Figure S6.** Expression of RAP2.12 in PIN2pro:PIN2-GFP lines crossed to wild type or to RAP2.12 OE2.

**Supplemental Table.** Primer names and sequences used in this study.

## ACKNOWLEDGMENTS

We are grateful to Michael J. Holdsworth (University of Nottingham, Loughborough, UK) for providing the *erfVII* mutant, to Jiri Friml (Institute of Science and Technology Austria, Austria) and Dominique van der Straeten (Ghent University, Belgium) for providing *pin* mutants, to Tim Ulmasov (Missouri University, Columbia, MO) for providing *DR5:GUS* seeds, to Tom Beeckman (Ghent University, Gent, Belgium) for sending us seeds of the DII-VENUS marker line, to Malcolm J. Bennett (University of Nottingham, Loughborough, UK) for providing *PIN2pro:PIN2-GFP* seeds, and to Angelika Mustroph (University Bayreuth, Germany) for providing seeds of the RAP2.12 OE2 line.

Received April 21, 2017; accepted July 7, 2017; published July 11, 2017.

## LITERATURE CITED

**Abas L, Benjamins R, Malenica N, Paciorek T, Wiśniewska J, Moulinier-Anzola JC, Sieberer T, Friml J, Luschnig C** (2006) Intracellular trafficking and proteolysis of the Arabidopsis auxin-efflux facilitator PIN2 are involved in root gravitropism. Nat Cell Biol **8:** 249–256

**Abbas M, Berckhan S, Rooney DJ, Gibbs DJ, Vicente Conde J, Sousa Correia C, Bassel GW, Marín-de la Rosa N, León J, Alabadí D, et al** (2015) Oxygen sensing coordinates photomorphogenesis to facilitate seedling survival. Curr Biol **25:** 1483–1488

**Abiko T, Kotula L, Shiono K, Malik AI, Colmer TD, Nakazono M** (2012) Enhanced formation of aerenchyma and induction of a barrier to radial oxygen loss in adventitious roots of *Zea nicaraguensis* contribute to its waterlogging tolerance as compared with maize (Zea mays ssp. mays). Plant Cell Environ **35:** 1618–1630

**Adamowski M, Friml J** (2015) PIN-dependent auxin transport: action, regulation, and evolution. Plant Cell **27:** 20–32

**Bailey-Serres J, Fukao T, Gibbs DJ, Holdsworth MJ, Lee SC, Licausi F, Perata P, Voesenek LA, van Dongen JT** (2012) Making sense of low oxygen sensing. Trends Plant Sci **17:** 129–138

**Baldwin KL, Strohm AK, Masson PH** (2013) Gravity sensing and signal transduction in vascular plant primary roots. Am J Bot **100:** 126–142

**Band LR, Wells DM, Fozard JA, Ghetiu T, French AP, Pound MP, Wilson MH, Yu L, Li W, Hijazi HI, et al** (2014) Systems analysis of auxin transport in the Arabidopsis root apex. Plant Cell **26:** 862–875

**Baster P, Robert S, Kleine-Vehn J, Vanneste S, Kania U, Grunewald W, De Rybel B, Beeckman T, Friml J** (2013) SCF(TIR1/AFB)-auxin signalling regulates PIN vacuolar trafficking and auxin fluxes during root gravitropism. EMBO J **32:** 260–274

**Blázquez MA, Soowal LN, Lee I, Weigel D** (1997) LEAFY expression and flower initiation in Arabidopsis. Development **124:** 3835–3844

**Blilou I, Xu J, Wildwater M, Willemsen V, Paponov I, Friml J, Heidstra R, Aida M, Palme K, Scheres B** (2005) The PIN auxin efflux facilitator network controls growth and patterning in Arabidopsis roots. Nature **433:** 39–44

**Boonsirichai K, Sedbrook JC, Chen R, Gilroy S, Masson PH** (2003) ALTERED RESPONSE TO GRAVITY is a peripheral membrane protein that modulates gravity-induced cytoplasmic alkalinization and lateral auxin transport in plant statocytes. Plant Cell **15:** 2612–2625

**Briggs WR** (2014) Phototropism: some history, some puzzles, and a look ahead. Plant Physiol **164:** 13–23

**Brunoud G, Wells DM, Oliva M, Larrieu A, Mirabet V, Burrow AH, Beeckman T, Kepinski S, Traas J, Bennett MJ, et al** (2012) A novel sensor to map auxin response and distribution at high spatio-temporal resolution. Nature **482:** 103–106

**Bui LT, Giuntoli B, Kosmacz M, Parlanti S, Licausi F** (2015) Constitutively expressed ERF-VII transcription factors redundantly activate the core anaerobic response in Arabidopsis thaliana. Plant Sci **236:** 37–43

**Clough SJ, Bent AF** (1998) Floral dip: a simplified method for Agrobacterium-mediated transformation of *Arabidopsis thaliana*. Plant J **16:** 735–743

**Dawood T, Rieu I, Wolters-Arts M, Derksen EB, Mariani C, Visser EJ** (2014) Rapid flooding-induced adventitious root development from preformed primordia in *Solanum dulcamara*. AoB Plants **9:** 6(0)

**Friml J, Benková E, Blilou I, Wisniewska J, Hamann T, Ljung K, Woody S, Sandberg G, Scheres B, Jürgens G, et al** (2002a) AtPIN4 mediates sink-driven auxin gradients and root patterning in Arabidopsis. Cell **108:** 661–673

**Friml J, Vieten A, Sauer M, Weijers D, Schwarz H, Hamann T, Offringa R, Jürgens G** (2003) Efflux-dependent auxin gradients establish the apical-basal axis of Arabidopsis. Nature **426:** 147–153

**Friml J, Wiśniewska J, Benková E, Mendgen K, Palme K** (2002b) Lateral relocation of auxin efflux regulator PIN3 mediates tropism in Arabidopsis. Nature **415:** 806–809

**Gälweiler L, Guan C, Müller A, Wisman E, Mendgen K, Yephremov A, Palme K** (1998) Regulation of polar auxin transport by AtPIN1 in Arabidopsis vascular tissue. Science **282:** 2226–2230

**Gasch P, Fundinger M, Müller JT, Lee T, Bailey-Serres J, Mustroph A** (2016) Redundant ERF-VII transcription factors bind to an evolutionarily conserved cis-motif to regulate hypoxia-responsive gene expression in Arabidopsis. Plant Cell **28:** 160–180

**Geisler M, Blakeslee JJ, Bouchard R, Lee OR, Vincenzetti V, Bandyopadhyay A, Titapiwatanakun B, Peer WA, Bailly A, Richards EL, et al** (2005) Cellular efflux of auxin catalyzed by the Arabidopsis MDR/PGP transporter AtPGP1. Plant J **44:** 179–194

**Gibbs DJ, Lee SC, Isa NM, Gramuglia S, Fukao T, Bassel GW, Correia CS, Corbineau F, Theodoulou FL, Bailey-Serres J, Holdsworth MJ** (2011) Homeostatic response to hypoxia is regulated by the N-end rule pathway in plants. Nature **479:** 415–418

**Gibbs DJ, Md Isa N, Movahedi M, Lozano-Juste J, Mendiondo GM, Berckhan S, Marín-de la Rosa N, Vicente Conde J, Sousa Correia C, Pearce SP, et al** (2014) Nitric oxide sensing in plants is mediated by proteolytic control of group VII ERF transcription factors. Mol Cell **53:** 369–379

**Habets ME, Offringa R** (2014) PIN-driven polar auxin transport in plant developmental plasticity: a key target for environmental and endogenous signals. New Phytol **203:** 362–377

**Hess N, Klode M, Anders M, Sauter M** (2011) The hypoxia responsive transcription factor genes ERF71/HRE2 and ERF73/HRE1 of Arabidopsis are differentially regulated by ethylene. Physiol Plant **143:** 41–49

**Hinz M, Wilson IW, Yang J, Buerstenbinder K, Llewellyn D, Dennis ES, Sauter M, Dolferus R** (2010) Arabidopsis RAP2.2: an ethylene response transcription factor that is important for hypoxia survival. Plant Physiol **153:** 757–772

**Karimi M, Inzé D, Depicker A** (2002) GATEWAY vectors for Agrobacterium-mediated plant transformation. Trends Plant Sci **7:** 193–195

**Kosmacz M, Parlanti S, Schwarzländer M, Kragler F, Licausi F, Van Dongen JT** (2015) The stability and nuclear localization of the transcription factor RAP2.12 are dynamically regulated by oxygen concentration. Plant Cell Environ **38:** 1094–1103

**Leitner J, Petrášek J, Tomanov K, Retzer K, Pařezová M, Korbei B, Bachmair A, Zažímalová E, Luschnig C** (2012) Lysine63-linked ubiquitylation of PIN2 auxin carrier protein governs hormonally controlled adaptation of Arabidopsis root growth. Proc Natl Acad Sci USA **109:** 8322–8327

**Licausi F, Kosmacz M, Weits DA, Giuntoli B, Giorgi FM, Voesenek LA, Perata P, van Dongen JT** (2011) Oxygen sensing in plants is mediated by an N-end rule pathway for protein destabilization. Nature **479:** 419–422

**Licausi F, van Dongen JT, Giuntoli B, Novi G, Santaniello A, Geigenberger P, Perata P** (2010) HRE1 and HRE2, two hypoxia-inducible ethylene response factors, affect anaerobic responses in Arabidopsis thaliana. Plant J **62:** 302–315

**Loreti E, van Veen H, Perata P** (2016) Plant responses to flooding stress. Curr Opin Plant Biol **33:** 64–71

**Marín-de la Rosa N, Sotillo B, Miskolczi P, Gibbs DJ, Vicente J, Carbonero P, Oñate-Sánchez L, Holdsworth MJ, Bhalerao R, Alabadí D, et al** (2014) Large-scale identification of gibberellin-related transcription factors defines group VII ETHYLENE RESPONSE FACTORS as functional DELLA partners. Plant Physiol **166:** 1022–1032

**Michniewicz M, Zago MK, Abas L, Weijers D, Schweighofer A, Meskiene I, Heisler MG, Ohno C, Zhang J, Huang F, et al** (2007) Antagonistic regulation of PIN phosphorylation by PP2A and PINOID directs auxin flux. Cell **130:** 1044–1056

**Müller A, Guan C, Gälweiler L, Tänzler P, Huijser P, Marchant A, Parry G, Bennett M, Wisman E, Palme K** (1998) AtPIN2 defines a locus of Arabidopsis for root gravitropism control. EMBO J **17:** 6903–6911

**Mustroph A, Lee SC, Oosumi T, Zanetti ME, Yang H, Ma K, Yaghoubi-Masihi A, Fukao T, Bailey-Serres J** (2010) Cross-kingdom comparison of transcriptomic adjustments to low-oxygen stress highlights conserved and plant-specific responses. Plant Physiol **152:** 1484–1500

**Mustroph A, Zanetti ME, Jang CJ, Holtan HE, Repetti PP, Galbraith DW, Girke T, Bailey-Serres J** (2009) Profiling translatomes of discrete cell populations resolves altered cellular priorities during hypoxia in Arabidopsis. Proc Natl Acad Sci USA **106:** 18843–18848

**Nakano T, Suzuki K, Fujimura T, Shinshi H** (2006) Genome-wide analysis of the ERF gene family in Arabidopsis and rice. Plant Physiol **140:** 411–432

**Nishimura T, Matano N, Morishima T, Kakinuma C, Hayashi K, Komano T, Kubo M, Hasebe M, Kasahara H, Kamiya Y, et al** (2012) Identification of IAA transport inhibitors including compounds affecting cellular PIN trafficking by two chemical screening approaches using maize coleoptile systems. Plant Cell Physiol **53:** 1671–1682

**Noh B, Murphy AS, Spalding EP** (2001) Multidrug resistance-like genes of Arabidopsis required for auxin transport and auxin-mediated development. Plant Cell **13:** 2441–2454

**Okada K, Ueda J, Komaki MK, Bell CJ, Shimura Y** (1991) Requirement of the auxin polar transport system in early stages of Arabidopsis floral bud formation. Plant Cell **3:** 677–684

**Ottenschläger I, Wolff P, Wolverton C, Bhalerao RP, Sandberg G, Ishikawa H, Evans M, Palme K** (2003) Gravity-regulated differential auxin transport from columella to lateral root cap cells. Proc Natl Acad Sci USA **100:** 2987–2991

**Péret B, Swarup K, Ferguson A, Seth M, Yang Y, Dhondt S, James N, Casimiro I, Perry P, Syed A, et al** (2012) AUX/LAX genes encode a family of auxin influx transporters that perform distinct functions during Arabidopsis development. Plant Cell **24:** 2874–2885

**Santner AA, Watson JC** (2006) The WAG1 and WAG2 protein kinases negatively regulate root waving in Arabidopsis. Plant J **45:** 752–764

**Sasidharan R, Bailey-Serres J, Ashikari M, Atwell BJ, Colmer TD, Fagerstedt K, Fukao T, Geigenberger P, Hebelstrup KH, Hill RD, et al** (2017) Community recommendations on terminology and procedures used in flooding and low oxygen stress research. New Phytol **214:** 1403–1407 10.1111/nph.14519

**Sauter M** (2013) Root responses to flooding. Curr Opin Plant Biol **16:** 282–286

**Schneider CA, Rasband WS, Eliceiri KW** (2012) NIH Image to ImageJ: 25 years of image analysis. Nat Methods **9:** 671–675

**Swarup K, Benková E, Swarup R, Casimiro I, Péret B, Yang Y, Parry G, Nielsen E, De Smet I, Vanneste S, et al** (2008) The auxin influx carrier LAX3 promotes lateral root emergence. Nat Cell Biol **10:** 946–954

**Swarup R, Kramer EM, Perry P, Knox K, Leyser HM, Haseloff J, Beemster GT, Bhalerao R, Bennett MJ** (2005) Root gravitropism requires lateral root cap and epidermal cells for transport and response to a mobile auxin signal. Nat Cell Biol **7:** 1057–1065

**Ulmasov T, Murfett J, Hagen G, Guilfoyle TJ** (1997) Aux/IAA proteins repress expression of reporter genes containing natural and highly active synthetic auxin response elements. Plant Cell **9:** 1963–1971

**van Dongen JT, Licausi F** (2015) Oxygen sensing and signaling. Annu Rev Plant Biol **66:** 345–367

**Voesenek LA, Bailey-Serres J** (2015) Flood adaptive traits and processes: an overview. New Phytol **206:** 57–73

**Wisniewska J, Xu J, Seifertová D, Brewer PB, Ruzicka K, Blilou I, Rouquié D, Benková E, Scheres B, Friml J** (2006) Polar PIN localization directs auxin flow in plants. Science **312:** 883–884

**Zhu J, Bailly A, Zwiewka M, Sovero V, Di Donato M, Ge P, Oehri J, Aryal B, Hao P, Linnert M, et al** (2016) TWISTED DWARF1 mediates the action of auxin transport inhibitors on actin cytoskeleton dynamics. Plant Cell **28:** 930–948